Fail-safe design for square vacuum-barrier windows

Tayyab I. Suratwala, John H. Campbell, William A. Steele, and Rusty A. Steele

University of California, Lawrence Livermore National Laboratory, P.O. Box 808, L-500, Livermore, California 94551-9900
(925) 422-6497

ABSTRACT

Laser-induced damage on the tensile side of vacuum-barrier fused silica optics can result in catastrophic fracture. This fracture can lead to two possible modes of failure: a benign failure resulting in a slow air leak into the vacuum chamber or an implosion. In previous work, we measured fracture in round vacuum windows and lenses and proposed a "fail-safe" design that would insure the benign failure mode by fracturing into only two parts, thus eliminating the possibility of implosion. In this paper we extend the previous work to include square vacuum-barrier windows and lenses. These results show that the expression developed describing the fracture area for round lenses:

$$A_f = 8.4\times10^{-5}\sigma_p{}^2 V_L$$

works equally well for square ones, where A_f is the generated fracture area (cm^2), σ_p the peak tensile stress (psi), and V_L the window or lens volume (liters). In addition, the effects of variable aperture size are considered, and we show that the maximum tensile stress (MPa) needed to generate a single, full-aperture fracture in a vacuum barrier optic scales as:

$$\sigma_p = \frac{K_f}{\sqrt{\ell_o}}$$

where K_f is an empirically-determined constant equal to 3.79 MPa • $m^{1/2}$ for round optics and 3.32 MPa • $m^{1/2}$ for square ones, and ℓ_o is the characteristic dimension (diameter or side length) of the window. Comparison of our results with recent work by others researching the conditions at which only one fracture will propagate in a glass plate show good agreement.

KEYWORDS: Glass fracture, Spatial filter lens, laser damage, fused silica, National Ignition Facility (NIF), glass vacuum window design, implosion

1. INTRODUCTION

Nova, Beamlet, and National Ignition Facility (NIF) are high-peak-power lasers that are being or will be used for Inertial Confinement Fusion (ICF) research at Lawrence Livermore National Laboratory (LLNL). These laser systems have several large vacuum chambers along the beam propagation path that use fused silica optics as vacuum barriers.[1-3] Laser induced damage on the tensile (vacuum) side of the optic can lead to catastrophic fracture. Catastrophic fracture occurs when a flaw on the tensile side of the optic exceeds the critical flaw size (based on Griffith's law[4]) and propagates one or more fractures completely through the optic. Catastrophic fracture can lead to two possible failure modes: a benign, slow air leakage into the vacuum chamber or an implosion. If the failure results in an implosion, the stored energy released can be tremendous for large vacuum chambers like the ones used on NIF (see Table 1). For example, the fracture and implosion of a vacuum window on the target chamber would release energy equivalent to 75 MJ. In comparison, the output of the NIF laser is only 1.8 MJ. Such an implosion would cause extensive collateral damage to the target chamber, target diagnostics and other laser optics and structures.

Table 1: The volume and stored energy for the three largest vacuum chambers on NIF.

Chamber Type	Vacuum Volume (m^3)	Stored Energy in Vacuum Chamber (MJ)
Cavity Spatial Filter	50	5
Transport Spatial Filter	93	9.3
Target	750	75

Previously, Beamlet and NOVA have experienced catastrophic fracture of the lenses on the vacuum spatial filters.[5,6] Table 2 summarizes the shape, dimensions, and peak stress on the affected optics. For comparison the size and peak stress for the vacuum barrier optics on the NIF are also shown. The catastrophic fracture of the Beamlet vacuum spatial filter lens,

SPIE Vol. 3492 • 0277-786X/99/$10.00

with a peak stress of 1490 psi, resulted in an implosion (~10 large fracture pieces). In contrast, the catastrophic fracture of Nova spatial filter lenses, with a peak stress of 810 psi, produced only one or two fractures. The two or three pieces of glass that remain after the fracture of the Nova lens, lock together resulting in a benign failure, i.e. a slow air leak. The number of fractures, and hence the mode of failure, are related to the peak stress on the glass part.

Table 2: Physical characteristics and peak stress in fused silica vacuum barrier optics used on LLNL fusion research lasers.

Laser	Aperture/ optic Shape	Optic Dimensions (cm) Length (side or diameter)	Thickness	Peak Stress (psi)	Number of major fractures	Failure mode
Nova	Round	52	3.7	810	1–2	Slow air leak
Beamlet	Round	61	3.5	1490	~9–11	Implosion
NIF	Square	43.4 - 45	4.3 – 4.6	500	—	—

The relationship between the peak stress and the number of fractures in round optics (windows and lenses) was investigated by Campbell et al.[5,6] An energy partition model was employed to relate the fracture area produced upon failure to the elastic stored energy in the glass part; specifically the greater the elastic stored energy in the stressed optic, the greater the number of fractures produced. (Note, the elastic stored energy considered here is not to be confused with the stored energy within the vacuum chamber that was discussed above.) Details of the energy partition model are outlined in the previous work.[5,6] The fracture area (A_f) was shown to be related to the peak tensile stress (σ_p) and the volume of the vacuum barrier optic (V_L):

$$A_f = k'\sigma_p^2 V_L \tag{1}$$

where k′ is an empirically derived constant that is primarily a function material properties. Because the fracture area is proportional to the square of the peak stress, then a modest change in the peak stress can result in a large change in fracture area.

In practice, one can reduce the peak stress and the fracture area by increasing the thickness of the vacuum barrier optic. This is illustrated by Eq. (2) that relates the peak stress to the optic thickness for a square glass plate that is simply supported at the edges:

$$\sigma_p = \frac{\beta q \ell^2}{t^2} \tag{2}$$

where β is at constant that is dependent on the geometry ($\beta = 0.2874$), q the applied load (MPa), ℓ the length of the side (m), and t the thickness of the glass plate (m).[7]

Unfortunately, increasing the thickness of the lens can adversely affect the beam quality at high laser intensities. This is because the increase in thickness increases the non-linear phase retardance, which in turn can amplify the noise intensity of the beam. The cumulative non-linear phase retardance is described by the so-called B integral:

$$\Delta B = \frac{2\pi}{\lambda}\int_0^L I\gamma dx \tag{3}$$

where ΔB is the cumulative retardance (radians), I the irradiance (GW/cm^2), and λ the laser wavelength (cm). L is the total thickness (cm) of optical material with nonlinear index coefficient, γ (cm^2/GW), through which the light traverses.[8-10] The general design rule is to limit ΔB to less than 2 radians so the noise amplification is insufficient to cause damage to the optics or adversely affect the focusability of the beam. Therefore, the thickness of the vacuum barrier optic is a trade-off between the demands of preventing an implosion versus minimizing non-linear noise growth.

Campbell et al.[5,6] used an energy partition model and data from fracture measurements of a number of Nova fused silica spatial filter lenses to determine k′ in Eq. (1), giving the following expression relating fracture area to the peak stress:

$$A_f = 8.4\times10^{-5}\frac{cm^2}{psi^2 liter}\sigma_p^2 V_L \tag{4}$$

3. RESULTS AND DISCUSSION

3.1 Glass fracture of square plates

Four different size square glass plates were tested to study the effect of peak stress on the number and area of fractures generated. The data and calculations from the fracture experiments are summarized in Table 3. A typical fracture pattern of a square plate is shown in Fig. 2. The crack originated from the laser-induced flaw at the center of the glass plate and propagated to the edges. The depth and width of the laser-induced damage flaw are reported in the second column of Table 3 and the maximum peak stress at the time of fracture is given in column three. Column four contains the number of fracture pieces, and column five lists the total measured fracture area, A_f, is given by:

$$A_f = 2\, t\, \ell_{tot} \tag{5a}$$

$$A_f = 2t \sum_{i=1}^{n} \ell_i \tag{5b}$$

where the total fracture length, ℓ_{tot} (m), is the sum of the lengths of all individual fractures, ℓ_i (m), and n is the total number of fractures. The factor of two in Eq. (5) accounts for the two surfaces created by each fracture.

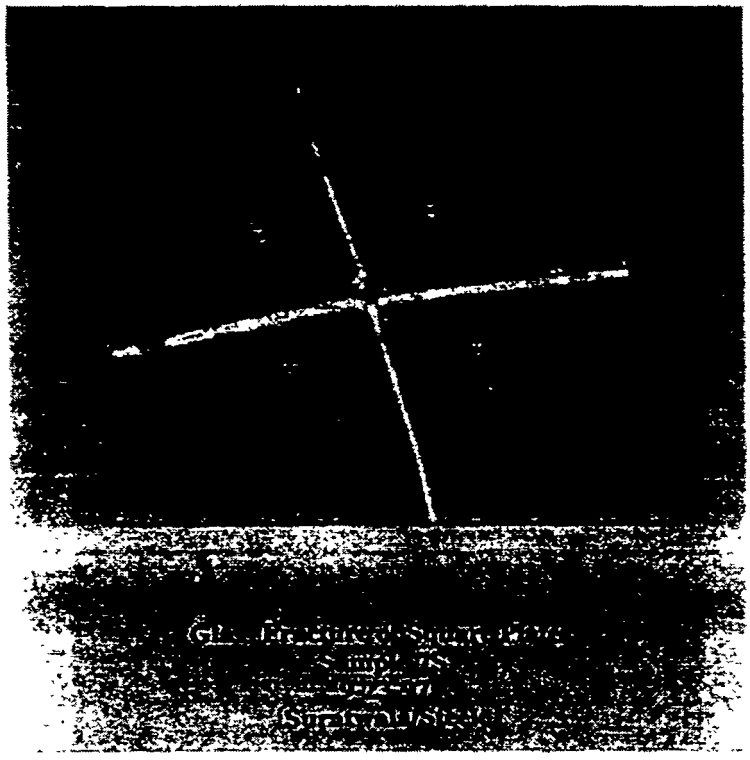

Figure 2: Photograph of a square glass plate ($12.5 \times 12.5 \times 0.6$ cm^3) that fractured at a vacuum load of 746 torr corresponding to a peak tensile stress of 1895 psi. Note the fracture initiated from the laser-induced damage spot.

The final column in Table 3 lists the predicted fracture area calculated using Eq. (4). The measured fracture areas are compared to the predicted values in Fig. 3. For comparison, data from the earlier study of round glass plates and lenses are also included on the graph. To within the scatter in the measurements, the agreement between the measured and predicted fracture area is quite good for both round and square glass plates. Thus the energy partition model appears valid for both square and round lenses.

Table 3: Summary of fracture data for square glass plates.

Effective Glass Size (cm)	Flaw Diameter/ Depth (mm)	Peak Stress at failure (psi / MPa)	Number of Pieces upon fracture	Measured Fracture Area (cm^2)	Predicted Fracture Area (cm^2)
12.5 × 12.5 × 0.6	4 / 5.9	1918 / 13.2	4	34	28
	4 / 5.9	1895 / 13.1	4	33	28
	4.5 / 1.8	1911 / 13.2	5	39	28
	3 / 1.5	1779 / 12.3	5	41	25
	2 / 2	1926 / 13.3	3	25	29
	3 / 2	1136 / 7.8[a]	3	25	10
12.5 × 12.5 × 0.5	3 / 0.5	1343 / 9.3[a]	3	22	11
	1 / 1	2631 / 18.1	4	30	44
	2 / 1	1192 / 8.2[a]	4	27	9
	1 / 2	2789 / 19.2	3	26	50
	2 / 1.5	2789 / 19.2	11	61	50
	1 / 1.8	2657 / 18.3	6	37	45
20.3 × 20.3 × 1.0	6 / 3.9	1704 / 11.8	3	86	103
	3.2 / 2.2	1680 / 11.6	6	144	100
	5.4 / 4.5	1701 / 11.7	4	101	103
	6.6 / 3.8	1703 / 11.7	3	70	103
	1.9 / 2.4	1703 / 11.7	3	72	103
	3.3 / 4.5	1644 / 11.3	3	71	96
	6.3 / 4	1601 / 11.0	2	44	91

[a] Actual chamber pressure may be lower than indicated by vacuum gauge due to possible flow restriction

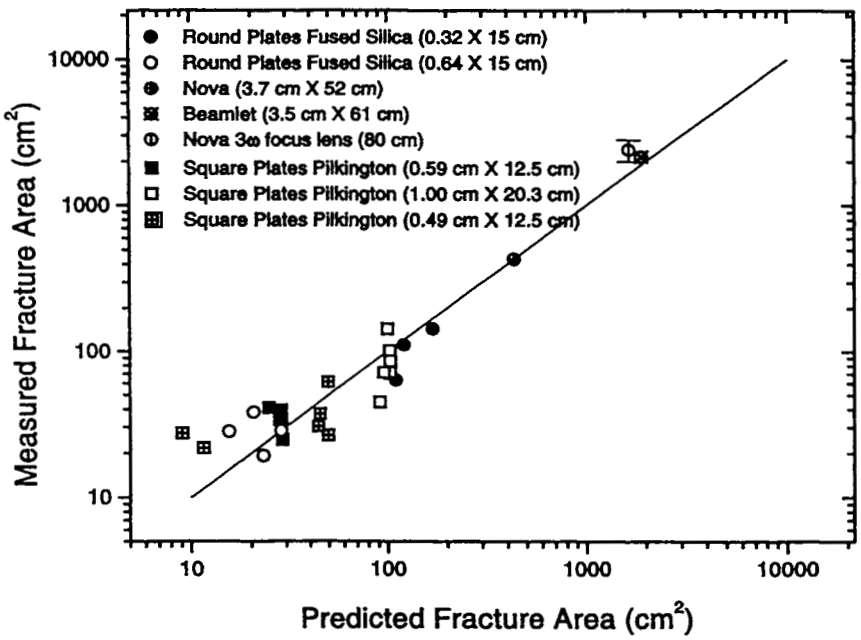

Figure 3: Measured vs. predicted fracture area for round glass plates (round symbols; data from Campbell et. al.[5]) and square glass plates (square symbols; data from this study). The predicted fracture area was calculated using Eq. (4).

3.2 Direction of fracture propagation in round and square plates

Fractures propagate in a direction determined by the gradient of the tensile stress ($\vec{\nabla} \bullet \sigma$) or, in other words, a direction normal the contours of equal tensile stress. For round plates, with uniform edge support and uniform surface loading (i.e. under vacuum), the maximum principle stress is the tangential ("hoop") stress. Thus, fractures will propagate radially across the disk, with one branch traveling in a path that is the shortest distance between the flaw and the edge and the other branch in approximately the opposite (180°) direction. For cases where the elastic stored energy is low (i.e. low stress) and only one full fracture is generated, the fracture will approximately bisect the plate (see, for example, Fig. 2 of reference 6). Fracture propagation in square plates follows the same principles. Figure 4 shows the iso-stress contours computed using standard stress-strain formulae[7] for a simply supported square glass plate under uniform vacuum load. The direction of propagation of a fracture is normal to the contours. Thus one can approximate the direction of fracture propagation from a damage induced flaw by first locating the flaw on the contour map and then simply drawing two lines radiating from the flaw in opposite directions and traveling normal to the contours. It is clear that fractures will deviate away from corners and, in principle, will intersect the edge of the plate near 90°. The fractured plate in Fig. 2 shows this behavior.

Close inspection of the initial direction of fracture propagation from a laser induced flaw generally shows that it is not in a direction normal to the static stress contours. This is because the localized stress generated during the damage event greatly exceeds the static stress. Consequently, the small fractures that radiate away from the damage site initially propagate in a direction determined by the gradient of the transient stress induced by the damage event. If the damage site grows to exceed the critical flaw size associated with the static stress field, then one or more of the small damage-induced fractures will continue to propagate. The fracture propagation will eventually bend in a direction normal to the static stress contours. An example of such behavior can clearly be seen in Fig. 2 of reference 5.

If the glass plate is highly stressed (high stored energy) then the propagating fractures soon reach a terminal velocity (about 1/3 to 1/2 sound speed in the glass) where crack growth becomes unstable.[12] At this point the crack will branch. Although there are some rules-of-thumb to predict crack branching angles[12-13], in general, accurately predicting the direction of crack propagation becomes much more difficult.

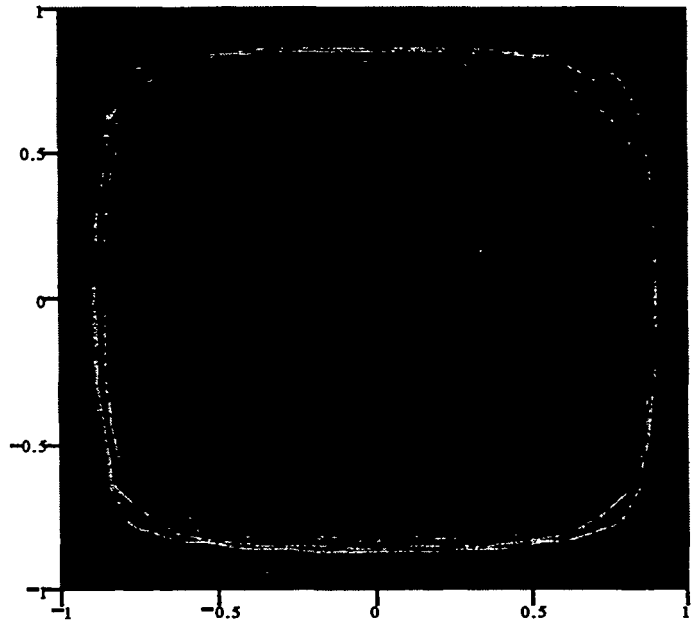

Figure 4: Iso-stress contours computed for a simply supported square glass plate ($12.5 \times 12.5 \times 0.6$ cm^3) under full vacuum load (14.7 psi) and having a Young's modulus and Poisson's ratio of 1.06×10^7 psi and 0.22, respectively. The peak tensile stress at the center of vacuum side of the plate is approximately 1900 psi. Each contour line represents a decrease of 100 psi from the center of the plate; the x and y dimensions are normalized to the plate half-width

3.3 Design criteria for a fail-safe vacuum barrier optic

In this section we use data from this study and previous work[5] to develop design criteria for "fail-safe" round and square vacuum barrier optics. The term fail-safe denotes any vacuum optic that, upon failure, produces no more than one full-aperture fracture. In other words, the optic will not implode if it fractures.

During fracture, the energy used to produce new surfaces is proportional to the elastic stored energy, E_s, in the material. In turn, the stored energy is related to the stress via the expression:

$$E_s = k \int_o^{V_L} \sigma \ \varepsilon \ dV \tag{6}$$

where σ is the stress (Pa), ε the strain (m), and V_L the integrated volume (m^3) of the elastic material under stress. The strain is related to stress via a Hook's law relationship:

$$\sigma = E\varepsilon \tag{7}$$

where E is Young's modulus (Pa). Substituting Eq. (7) into (6) and integrating gives the well known expression:

$$E_s = \frac{k\sigma_p^2 V_L}{E} \quad . \tag{8}$$

We have shown in this study and our previous work that the fraction (f_o) of elastic stored energy used to generate new surfaces (fractures) is nearly constant for a wide range of round and square optic sizes (Fig. 3). Thus, the surface energy produced during fracture (E_f) can be related to the total elastic stored energy by the expression:

$$E_f = f_o E_s \qquad \text{or} \tag{9a}$$

$$E_f = f_o \frac{k\sigma_p^2 V_L}{E} \tag{9b}$$

where all the terms have been previously defined. Note that E_f can also be written as:

$$E_f = \gamma_f A_f \tag{10}$$

where γ_f (J/cm^2) is the material fracture surface energy. Equating Eq. (9) and (10) and rearranging gives an expression for the fracture area as a function of the optic volume, peak tensile stress, and the material properties:

$$A_f = \frac{f_o k}{\gamma_f E}\sigma_p^2 V_L \tag{11}$$

Equation (11) is the same as Eq. (1) where k′ is used to represent the set of constants ($f_o k/\gamma_f E$). We have measured the fracture area produced as a function of peak stress and optic volume and determined at a value of k′ equal to 8.4×10^{-5} cm^2/psi^2 liter.

By making use of Eq. (5), Eq. (11) can also be written in terms of the total fracture length (ℓ_{tot})

$$\ell_{tot} = \frac{k'\sigma_p^2 V_L}{2t} \tag{12}$$

where we have substituted k′ for ($f_o k/\gamma_f E$). Equation 12 can be further simplified by expressing the volume of the optic in terms of its dimensions:

$$V_L = c\ell_o^2 t \tag{13}$$

where ℓ_o is the characteristic dimension (diameter or length) and c equals $\pi/4$ or 1, respectively, for a round or square optic. Substitution of Eq. (13) in (12) leads to the very useful relationship for total fracture length as a function of the peak stress, optic shape, and characteristic dimension:

$$\ell_{tot} = \left(\frac{k'c}{2}\right)\sigma_p^2 \ell_o^2 \tag{14}$$

It is useful to think of the total fracture length, ℓ_{tot}, in terms of multiples of the optic dimension:

$$n_f = \frac{\ell_{tot}}{\ell_o} \tag{15}$$

where n_f is the number of equivalent "full dimension" fractures. Combining Eq. (14) and (15) leads to the useful design equation:

$$n_f = \left(\frac{k'c}{2}\right)\sigma_p^2 \ell_o \tag{16}$$

Recall that the design criteria for a "fail-safe" lens is that n_f not exceed one or, expressed in terms of the limiting peak stress, is:

$$\sigma_p \le \left(\frac{k'c\ell_o}{2}\right)^{-1/2} \tag{17}$$

Upon substituting the experimentally-determined value of k', Eq. (17) can be simply written for round optics as:

$$\sigma_p \le \frac{3.79}{\sqrt{d}}\,\text{MPa} \bullet m^{1/2} = \frac{551}{\sqrt{d}}\,\text{psi} \bullet m^{1/2} \tag{18a}$$

where d is the diameter and for square optics:

$$\sigma_p \le \frac{3.32}{\sqrt{s}}\,\text{MPa} \bullet m^{1/2} = \frac{488}{\sqrt{s}}\,\text{psi} \bullet m^{1/2} \tag{18b}$$

where s is the length of the side width. Note that s and d refer to the distances across the optic between the vacuum mounting surfaces.

The peak tensile stresses, calculated using Eqs. (18a) and (18b), are plotted as a function of lens size in Fig. 5. The corresponding peak stresses for the glass sizes used in the study and for the glass sizes used in LLNL ICF lasers (Nova, Beamlet and NIF [planned]) are also marked in the figure.

The peak tensile stress required to propagate one full-diameter fracture in a 61-cm-diameter Beamlet vacuum spatial filter lens is about 700 psi based on Eq. (18a); the actual peak stress on the lens was 1490 psi. Thus it is clear such an optic has a high risk of imploding upon catastrophic fracture and, indeed, that failure mode was observed. In sharp contrast, the square 42.6-cm NIF spatial filter lens would require a peak stress of nearly 750 psi to propagate one full-width fracture; the design stress on the lens is set at 500 psi, well below the one-fracture limit, insuring the lens will not implode.

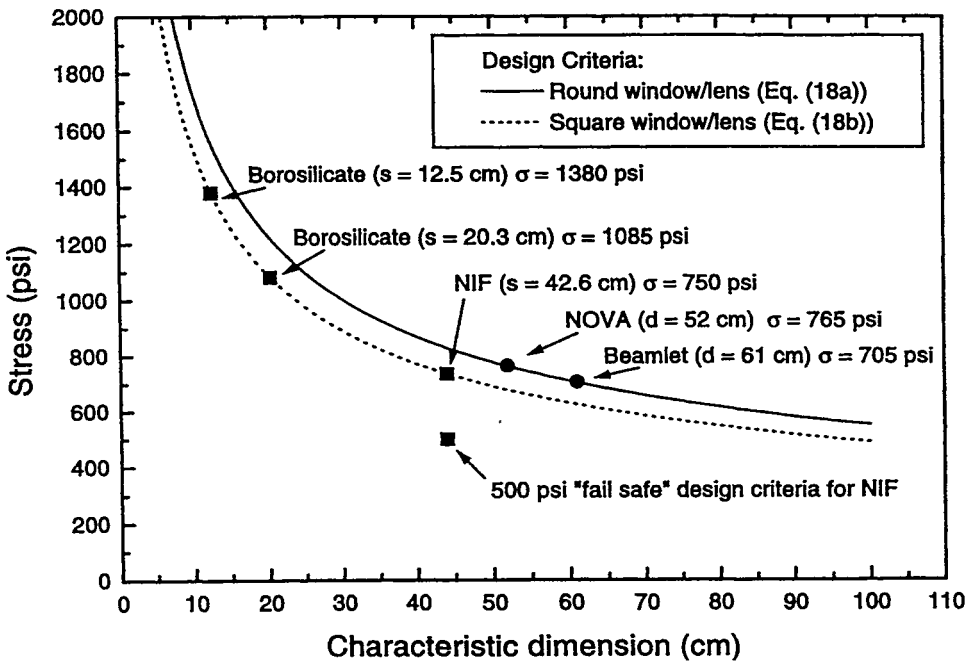

Figure 5: Predicted peak tensile stress required to produce one full-diameter fracture in square and round vacuum barrier optics; the prediction is based on Eq. (18a) and (18b).

3.4 Other studies of single fracture generation

Glass fractologists have long sought to develop empirically-based methods for diagnosing the conditions under which glass parts fail. Such diagnostic methods are used during post-failure examination of the fracture surfaces. One useful diagnostic method is to examine the distance between the initiating (critical) flaw and the first crack branching point. Studies have shown that this distance is related to the stress at failure via the expression[13–16]:

$$\sigma_f = \frac{K_f}{\sqrt{2\ell_b}} \tag{19}$$

where K_f (MPa • $m^{1/2}$) is an empirically-derived constant, σ_f the peak stress (MPa) at failure, and ℓ_b is the distance (m) to the first branching point. Thus, by measuring the first branching distance, one can estimate the value of the stress at the time of failure. The first branching distance is often termed the fracture "mirror radius" because of it's distinct physical appearance on the fracture surface.[12–14]

Quinn recently suggested[15] that the first branching distance (i.e. mirror radius) can be thought of as the maximum radius of a glass part that would generate only one fracture at the corresponding stress (Eq. (19)). Thus it is interesting to compare K_f, determined by fracture mirror studies, with the value of K_f measured in this work (see Table 2). The agreement is quite good. Note that this is indeed remarkable; it implies that one simple scaling relationship can be used to describe single fracture generation in round or square glass parts ranging in size from a few hundred microns up to a meter.

Table 4: Value of K_f based on data collected by different researchers using different measurement methods

Source	K_f (MPa • $m^{1/2}$)	Measurement
Quinn[15]	3.22	Mirror radius
Orr[16]	3.03	Mirror radius
Present study: round	3.79	Fracture area
: square	3.32	Fracture area

3.5 500 psi Design criteria for NIF vacuum barrier optics

We have chosen the peak design stress for the NIF vacuum barrier optics to be 500 psi despite the prediction of a "fail-safe" stress of 750 psi based on Eq. (18b). There are two reasons for this: the first is to account for the error bars in our measurement of the fracture area and the second is to compensate for the possibility of secondary fracture.[5] Secondary fracture refers to crack growth that occurs subsequent to the initial fracture event and is driven by the redistribution of the stress in response to the change in boundary conditions. For example, after a square or round optic breaks into two parts, the remaining two pieces may remain under load (if the gas leak is slow) and each piece now develops a new stress distribution in response to the unsupported fracture edge.

Using finite element analysis, the stress distribution was calculated for a NIF target chamber window before and after primary fracture (see Fig. 6). The peak tensile stress in each of the two halves increased from 499 psi to 812 psi, an increase of a factor of 1.6. After primary fracture a portion of the initial flaw may remain in both glass pieces. Therefore secondary fractures will occur in either piece if the critical stress (based on Griffith's Law[4]) is exceeded. Note that the change in the stress profile after primary fracture leads to an increase in the elastic stored energy in the glass part, and hence a greater likelihood of creating more fracture area. To minimize the possibility of secondary fracture, the peak fail-safe design stress predicted by Eq. (18b) was reduced from 750 psi to a value of 500 psi. The new 500 psi criteria can be considered as the maximum peak stress required to prevent both primary and secondary fracture.

Finally, another safety factor built into the laser system design is a diagnostic that can detect damage on the optics. With a 500-psi peak stress the critical flaw size is approximately 1.5 cm. The diagnostics on NIF are capable of detecting flaws less than 1 mm in size, hence the flaw will be easily detected well before any type of catastrophic fracture can occur.

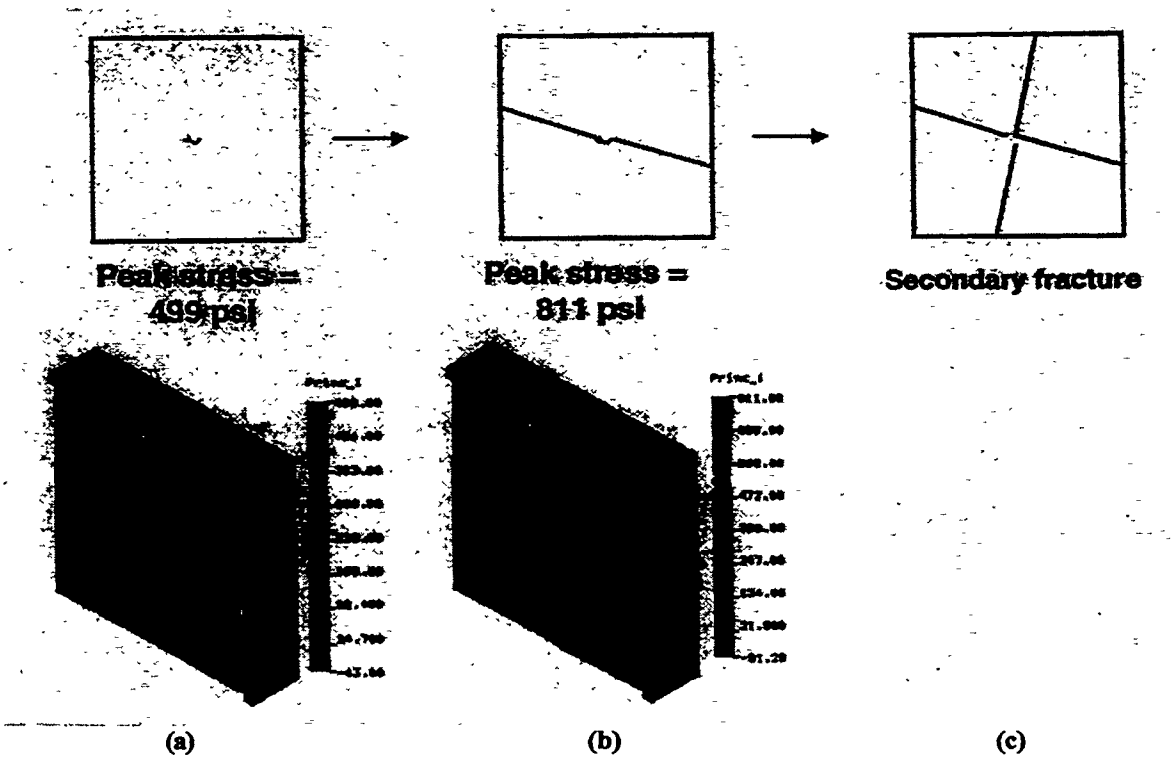

Figure 6: Illustration of secondary fracture and finite element analysis of the stress distribution in target vacuum windows (a) before primary fracture, (b) after primary fracture, and (c) after secondary fracture. The peak stress before is 499 psi and after is 812 psi.

4. ACKNOWLEDGMENTS

The authors gratefully acknowledge Kip Hamilton for performing the finite element analysis on the NIF Target Vacuum Barriers. Work performed under the auspices of the US Department of Energy by Lawrence Livermore National Laboratory under contract No. W-7405-Eng-48.

5. REFERENCES

1. B. M. VanWonterghem, J. R. Murray, J. H. Campbell, D. R. Speck, C. E. Barker, I. C. Smith, D. F. Browning and W. C. Behrendt, *Applied Optics* **36**, 4932–4953 (1997).
2. "National Ignition Facility Conceptual Design Report" *UCRL-PROP-117093* (Lawrence Livermore National Laboratory, 1994).
3. J. Hunt, D. Speck, *Opt. Eng.* **28**, 461-468 (1989).
4. A. A. Griffith, *Philos. Trans. R. Soc.* **A221**, 163 (1920).
5. J. Campbell, P. Hurst, D. Heggins, W. Steele, S. Bumpas, *SPIE* **2986**, 106-125 (1996).
6. J. Campbell, G. Edwards, J. Marion, *SPIE* **2633**, 522-523 (1995).
7. R. Roark, W. Young, *Formulas for Stresses and Strain* (New York, 1982).
8. W. Simmons, J. Hunt, W. Warren, *IEEE J. Quantum Electron* **QE-17**, 1727-1744 (1981).
9. J. Hunt, J. Glaze, W. Simmons, P. Renard, *Appl Opt.* **17**, 2053-2057 (1978).
10. J. Trenholme, "1975 Laser Program Annual Report" *UCRL-50021-75* (1975).
11. Timoshenko, *Theory of Plates and Shells* (1959).
12. V.D. Frechette, *Failure Analysis of Brittle Materials*, Am. Ceram. Soc. Press, Ohio (1990) p 28.
13. J. Mencik, "Strength and Fracture of Glass and Ceramics", Elsevier, New York (1992).
14. S. W. Freiman, "Fracture Mechanics of Glass", Chap. 2, *Glass: Science and Technology*, Vol. 5, D. R. Uhlmann and N. D. Kreidl (eds.), Academic Press (1980), New York.
15. J. Quinn, *Key Engineering Materials* **132-136**, 492-495 (1997).
16. L. Orr, *ASTM Materials Research and Standards* **12**, 21-23 (1972).